Robust filtering for joint state parameter estimation for distributed mechanical systems

Dominique Chapelle, Philippe Moireau, Patrick Le Tallec

Robust filtering for joint state-parameter estimation in distributed mechanical systems

Dominique Chapelle†,*, Philippe Moireau†, Patrick Le Tallec‡
†INRIA, B.P. 105, 78153 Le Chesnay cedex, France
‡Ecole Polytechnique, 91128 Palaiseau cedex, France

DCDS-A, 23(1-2): 65-84, 2009, doi:10.3934/dcds.2009.23.65

Abstract

We present an effective filtering procedure for jointly estimating state variables and parameters in a distributed mechanical system. This method is based on a robust, low-cost filter related to collocated feedback and used to estimate state variables, and an H^∞ setting is then employed to formulate a joint state-parameter estimation filter. In addition to providing a tractable filtering approach for an infinite-dimensional mechanical system, the H^∞ setting allows to consider measurement errors that cannot be handled by Kalman type filters, e.g. for measurements only available on the boundary. For this estimation strategy a complete error analysis is given, and a detailed numerical assessment – using a test problem inspired from cardiac biomechanics – demonstrates the effectiveness of our approach.

1 Introduction

The formulation and optimization of filtering procedures aiming at estimating both the state variables and the parameters of a dynamical system has been an active field of research for several decades, and some effective strategies have been proposed, see e.g. [8, 10] and their references. However, these procedures have long been restricted to systems with only a very limited number of state variables and parameters – due to the induced size of filter matrices to be manipulated – making them out of reach for the estimation of systems based on partial differential equations. Only recently have some so-called "reduced rank filtering" procedures been proposed, in order to deal with such large systems by reducing the size of the space of "uncertain variables" considered [11]. In many infinite dimensional systems, however, this uncertainty space is *intrinsically* very large, hence generic rank reduction is not applicable.

In [9] we have proposed a new filtering procedure based on a two-stage strategy:

1. a physics-based state filter – related to feedback stabilization – allows to estimate the state variables very effectively, namely, at a computational cost comparable to standard numerical simulations of the system, assuming that the parameters are known;

2. a second filter – based on optimal filtering methods – is applied in order to jointly estimate the parameters and the state.

*Corresponding author: dominique.chapelle@inria.fr

We have also shown that this strategy is closely related to reduced rank procedures, the effect of the first stage state filter being in essence to circumscribe the uncertainty to the parameter space – which is usually much "smaller" than the parameter space, indeed. In distributed mechanical systems in particular, the state filter can rely on collocated feedback, and we have demonstrated the effectiveness of our approach using a test problem inspired from cardiac mechanics and imaging. Nevertheless, an important limitation of this approach is that the second stage optimal filter derivation is based on the assumption that all "static" uncertainties – namely, essentially initial conditions – are Gaussian probabilistic variables and that "dynamic" uncertainties – in particular measurement errors – are white noises. This clearly represents a limitation as other types of uncertainty modeling – whether probabilistic or deterministic – may be more relevant for specific systems and according to the metrology considered. As a matter of fact, if the measurement used is restricted to the boundary of a mechanical system and with a collocated force feedback, it can be shown (see Section 2) that white noise errors lead to non-bounded mean mechanical energies, which of course is not admissible.

Therefore, in this paper we formulate a new filter based on a similar two-stage approach, albeit obtained by recasting the estimation problem in a robust (H^∞) filtering framework. Although this setting is quite drastically different from [9], it leads to similar filter equations, with an additional term which is straightforward to implement. More fundamentally, it allows to consider *general uncertainties*, and provides a performance bound that guarantees a given robustness criterion – in the usual H^∞ form – is fulfilled.

The outline of the paper is as follows. In Section 2 we analyse the effect of a white noise loading on the boundary of a mechanical system, as part of the above-mentioned motivation of our approach. Section 3 is devoted to the presentation of the system on which estimation is to be performed, with the detailed definition of a test problem. Then, in Section 4 we introduce the state estimation strategy and we derive the corresponding estimation error equations, before performing some numerical assessments of this error. Finally, we present in Section 5 the formulation of the joint state-parameter estimation procedure with detailed mathematical analyses and numerical testing, before giving some concluding remarks in Section 6.

2 Preliminary: energy induced by a white noise loading in a mechanical system

In order to explain why we cannot deal with distributed mechanical systems submitted to white noise type excitations on their boundary we consider the following basic example of a conservative system:

$$M\ddot{Y} + KY = \dot{F}, \tag{2.1}$$

where F represents a field – smooth in the space variables – that may be either 3D-distributed or concentrated on the boundary, and corresponding to a Wiener process in the time variable, so that $\dot{F}$ is a white noise. Note that to avoid undue technicalities we adopt here a finite dimensional description, but a similar argument also applies – at least formally – with infinite-dimensional operators. In the state space formalism the above dynamical equation can be rewritten as

$$\dot{X} = AX + \dot{R}, \tag{2.2}$$

with

$$X = \begin{pmatrix} Y \\ \dot{Y} \end{pmatrix}, \quad A = \begin{pmatrix} 0 & I \\ -M^{-1}K & 0 \end{pmatrix}, \quad R = \begin{pmatrix} 0 \\ M^{-1}F \end{pmatrix}. \tag{2.3}$$

Note that $\dot{R}$ is also a white noise. Let us compute the mean energy of the state X along time, using the energy norm matrix defined by

$$N = \frac{1}{2}\begin{pmatrix} K & 0 \\ 0 & M \end{pmatrix}.$$

Introducing the semi-group $\mathcal{T}^h(t)$ generated by A so that

$$X(t) = \mathcal{T}^h(t)X(0) + \int_0^t \mathcal{T}^h(t-s)\dot{R}(s)\,ds, \tag{2.4}$$

some simple algebra leads to

$$\begin{aligned} \mathbb{E}(\|X\|_{\mathcal{E}}^2) &= \mathbb{E}(X^T N X) \\ &= X(0)^T\mathcal{T}^h(t)^T N\mathcal{T}^h(t)X(0) + \int_0^t\int_0^t \mathbb{E}\big(\dot{R}(\tau)^T\mathcal{T}^h(t-\tau)^T N\mathcal{T}^h(t-s)\dot{R}(s)\big)\,d\tau ds, \end{aligned} \tag{2.5}$$

Since the mechanical system is conservative the first term gives

$$X(0)^T\mathcal{T}^h(t)^T N\mathcal{T}^h(t)X(0) = \|\mathcal{T}^h(t)X(0)\|_{\mathcal{E}}^2 = \|X(0)\|_{\mathcal{E}}^2. \tag{2.6}$$

Moreover, denoting by Q_R the covariance of the Wiener process R and using

$$\dot{R}(\tau)^T\mathcal{T}^h(t-\tau)^T N\mathcal{T}^h(t-s)\dot{R}(s) = \mathrm{Tr}\big(\dot{R}(s)\dot{R}(\tau)^T\mathcal{T}^h(t-\tau)^T N\mathcal{T}^h(t-s)\big),$$

together with $\mathbb{E}(\dot{R}(s)\dot{R}(\tau)^T) = Q_R\,\delta(t-s)$, we infer

$$\begin{aligned} \mathbb{E}(\|X\|_{\mathcal{E}}^2) &= \|X(0)\|_{\mathcal{E}}^2 + \int_0^t \mathrm{Tr}\big(Q_R\mathcal{T}^h(t-\tau)^T N\mathcal{T}^h(t-\tau)\big)\,d\tau, \\ &= \|X(0)\|_{\mathcal{E}}^2 + \int_0^t \mathbb{E}\big(R(\tau)^T\mathcal{T}^h(t-\tau)^T N\mathcal{T}^h(t-\tau)R(\tau)\big)\,d\tau, \\ &= \|X(0)\|_{\mathcal{E}}^2 + \int_0^t \mathbb{E}\big(R(\tau)^T N R(\tau)\big)\,d\tau, \\ &= \|X(0)\|_{\mathcal{E}}^2 + \int_0^t \tau\,\mathrm{Tr}(Q_R N)\,d\tau, \\ &= \|X(0)\|_{\mathcal{E}}^2 + \frac{t^2}{2}\,\mathrm{Tr}(Q_R N). \end{aligned} \tag{2.7}$$

Note now that

$$\mathrm{Tr}(Q_R N) = \mathbb{E}(F^T M^{-1} F), \tag{2.8}$$

so that the mean energy is bounded – or in the discrete framework uniformly bounded with respect to the discretization – only when F corresponds space-wise to a field belonging to the dual of $L^2(\Omega)$. This holds when the loading is smoothly 3D-distributed, but of course not when it is concentrated on the boundary. Hence, applying a boundary-concentrated white noise as a loading in a general mechanical system is not admissible from the energy point of view.

3 Problem statement

3.1 General framework

We consider a mechanical system in the realm of solid or structural continuum mechanics, where the acceleration field inside the body is given by the imbalance between internal stresses and external forces. When x denotes the state vector including displacements $\underline{y}$ and velocities $\underline{\dot{y}}$, such systems are described in a linear framework by a dynamical system – underlied by partial differential equations – written in the following generic form

$$\begin{cases} \dfrac{dx}{dt} = \mathcal{A}x + \mathcal{R} \\ x(0) = x_0 + \zeta_x \end{cases} \tag{3.1}$$

where $\mathcal{A}$ is a linear differential operator generating a continuous semi-group, and $\mathcal{R}$ a source term. More specifically, this equation expresses the conservation of linear momentum, completed by the identity relating the velocity and the time derivative of displacement, namely, in a weak form,

$$\int_\Omega \rho \frac{d\underline{\dot{y}}}{dt} \cdot \underline{\delta y}\, d\Omega = \int_\Omega \rho \underline{\dot{y}} \cdot \underline{\delta y}\, d\Omega, \quad \forall \underline{\delta y} \tag{3.2}$$

$$\int_\Omega \rho \frac{d\underline{\dot{y}}}{dt} \cdot \underline{\delta y}\, d\Omega = -\int_\Omega \underline{\underline{\Sigma}}(\underline{y}, \underline{\dot{y}}) : \underline{\underline{\delta e}}\, d\Omega + \int_\Omega \underline{f} \cdot \underline{\delta y}\, d\Omega, \quad \forall \underline{\delta y} \tag{3.3}$$

Here Ω represents the geometrical domain of the system, ρ the mass per unit volume, $\underline{\underline{\Sigma}}$ the second Piola-Kirchhoff stress tensor, $\underline{\delta y}$ an arbitrary test function in the displacement space with $\underline{\underline{\delta e}}$ the corresponding infinitesimal variation for the Green-Lagrange strain tensor, and $\underline{f}$ the applied loading (taken here as a 3D distributed field to fix the ideas). Hence, in System (3.1) x denotes the state variable $(\underline{y} \quad \underline{\dot{y}})^T$. Assuming *small displacements*, we can identify $\underline{\underline{\delta e}}$ with the symmetric part of the gradient $\nabla \underline{\delta y}$, and take $\underline{\underline{\Sigma}}$ – which can then be identified with the Cauchy stress tensor – as a linear function of x. We are thus led to the *linear* operator $\mathcal{A}$. The differential system considered is of infinite dimension, its unknowns being the displacement and velocity fields at each point of the continuous body.

In the above system, ζ_x represents the unknown part in the initial condition $x(0)$. Likewise, we assume that $\mathcal{A}$ and $\mathcal{R}$ depend on a set of parameters in the form

$$\theta = \theta_0 + \zeta_\theta, \tag{3.4}$$

in which ζ_θ is undetermined. Our objective is to obtain a joint estimation of the unknown quantities ζ_x and ζ_θ, based on measurements available for the system. These measurements are assumed to be given by

$$Z = \mathcal{H}x + \chi$$

where $\mathcal{H}$ is a linear operator referred to as the observation operator, and χ denotes an error introduced by the measurement procedure (detection, sampling...). We also introduce

$$\bar{Z} = \mathcal{H}x \tag{3.5}$$

to represent an "exact measurement" which of course is never available in practice. More specifically, in the whole paper the measurements considered will be the velocities taken in a subpart Γ_m of the domain boundary $\partial\Omega$. Namely, $\mathcal{H}x = (0\ \mathcal{H}^v)(\underline{y}\ \underline{\dot{y}})^T$ consists of the trace of the velocity field on Γ_m. Note that, in general, the regularity required to obtain such a trace is not naturally induced by the mechanical variational formulation (3.2)-(3.3), hence in the sequel we will *assume* that we have sufficient regularity in the solution for this trace to lie in $L^2(\Gamma_m)$.

3.2 Modelling and discretization

Our observer approach relies on a discretized version of the above reference model, typically obtained by a finite element approximation of the variational formulation. Hence, we introduce A and R as the discrete counterparts of $\mathcal{A}$ and $\mathcal{R}$ obtained from this variational approximation, namely,

$$A = \begin{pmatrix} 0 & I \\ -M^{-1}K & -M^{-1}C \end{pmatrix}, \quad R = \begin{pmatrix} 0 \\ M^{-1}F \end{pmatrix}, \tag{3.6}$$

when M, C, K and F respectively denote the mass, damping and stiffness matrices and the consistent force vector, see e.g. [3, 5]. We also define H as the discrete observation operator, namely, the operator giving the trace on Γ_m of the velocity part of a discrete state vector. Since H only acts on velocities – like the continuous observation operator $\mathcal{H}$ – we will also use the expression

$$H = (0 \quad H^v) = (0 \quad \mathfrak{I}_\Gamma T_\Gamma),$$

where T_Γ is defined as a matrix that selects the degrees of freedom located on Γ_m, and $\mathfrak{I}_\Gamma$ as the operator that interpolates a surface field from these degrees of freedom.

3.3 Model problem

In order to illustrate and assess our estimation procedures, we will consider an example problem inspired from biomechanics and representing a simplified cardiac ventricle. This model problem was already considered in [9], but for completeness we now summarize its definition.

The geometry of our example problem is depicted in Figure 1, and the characteristic dimensions of this object are – indeed – comparable to those of a human left ventricle. We thus resort to cardiac terminology to refer to the two extremities of the object, namely "apex and base" (see Figure). The system is clamped over the planar surface at the base, and activated by a planar wave of prestress – representing electrical activation – traveling from apex to base at wave speed $c = 0.5$ m.s^{-1}, which means that it takes 0.2 s for the wave to reach the base. The wave shape itself is shown in Figure 2. The resulting prestress state is assumed to be isotropic and gives an external virtual work defined by

$$\delta\mathcal{W}^{PS} = \sum_{1\leq i\leq 17} \int_{\Omega_i^{AHA}} \theta_i \sigma_0 w(x_3 - ct)\ \mathrm{Tr}(\delta\nabla\underline{y})\, d\Omega = \delta Y^T \cdot R, \tag{3.7}$$

where the subdivision of the solid domain into 17 sub-regions is similar to the subdivision of the left ventricle advocated by the American Heart Association, see [1]. In the case of our simplified geometry this subdivision is depicted in Fig. 1. In the above expression σ_0 denotes a constant contractility parameter, and θ_i a multiplicative coefficient that may take a different value in the range $[0, 1]$ within each AHA region to represent pathological contraction. Namely, setting $\theta_i < 1$ in a given region corresponds to a simplified model of infarcted tissue in that area, hence the parameters $(\theta_i)_{1\leq i\leq 17}$ represent the quantities to be estimated for diagnosis purposes. In our reference simulations we take all these parameters to be 1 (healthy value) except for

$$\theta_{14} = 0.5, \tag{3.8}$$

see Figure 3.

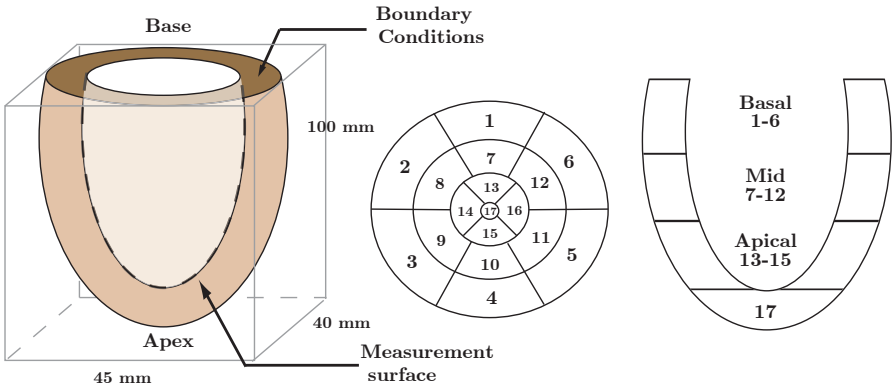

Figure 1: Model geometry (left) and AHA regions (center and right)

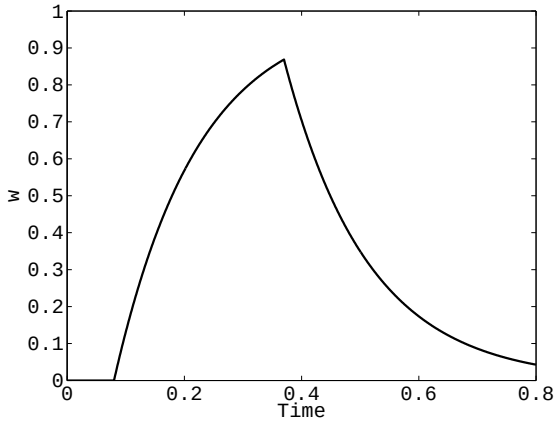

Figure 2: Activation profile w

Our simulations will correspond to an isotropic viscoelastic material in *linear analysis*, with material parameters given by

$$E_i = 12.6\,10^3\,\text{Pa}, \quad \nu_i = 0.3, \quad \eta_i = 0.227\,\text{s} \quad \forall i \in \{1,\dots,17\}, \tag{3.9}$$

and respectively denoting Young's modulus, the Poisson ratio and a viscoelastic coefficient associated with the pseudo-potential

$$W^v = \eta_i \left(\frac{\lambda_i}{2} (\text{Tr}\, \underline{\underline{\dot{\varepsilon}}})^2 + \mu_i \,\text{Tr}(\underline{\underline{\dot{\varepsilon}}}^2) \right), \quad \forall i \in \{1,\dots,17\},$$

where λ_i et μ_i are the Lamé constants derived from E_i and ν_i, and

$$\underline{\underline{\varepsilon}} = \frac{1}{2}(\nabla \underline{y}^T + \nabla \underline{y})$$

denotes the linearized strain tensor approximating – at the first order – the Green-Lagrange deformation tensor in the small displacements framework. Note that this viscoelastic contribution corresponds to

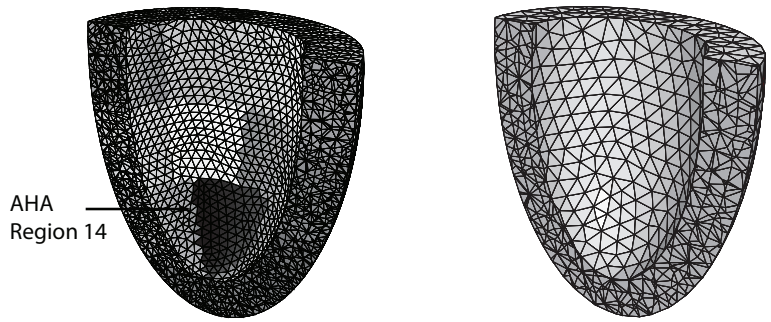

Figure 3: Reference mesh with 'infarcted' region (left) - 'Desired' mesh to be used in estimation (right)

stiffness-based Rayleigh proportional damping. This leads to the following constitutive law to be taken into account in the variational formulation

$$\underline{\underline{\Sigma}} = \lambda_i \, \mathrm{Tr}(\underline{\underline{\varepsilon}} + \eta_i \underline{\underline{\dot{\varepsilon}}}) \underline{\underline{1}} + 2\mu_i (\underline{\underline{\varepsilon}} + \eta_i \underline{\underline{\dot{\varepsilon}}}). \tag{3.10}$$

Also, volumic mass is set as $\rho = 10^3 \, \mathrm{kg} \cdot \mathrm{m}^{-3}$, a standard value for biological tissues.

The measurements used in the estimation procedures will be provided by a "reference model" given by a rather fine finite element discretization of the above object. The corresponding mesh is displayed in Figure 3 and features nearly 40000 degrees of freedom. The observer itself will be based on coarser discretizations, where the adequate mesh size will be a matter of discussion in the sequel. In all our simulations we used for time discretization the energy-conserving Newmark algorithm with time step $\Delta t = 1$ ms. This time step is adequate for accurately representing the first 1000 eigenmodes of the system with at least 20 time steps per modal period, but is primarily determined in relation to the activation wave velocity.

In our numerical testing of the estimation procedures, the surface Γ_m on which velocity measurements are obtained is the internal boundary of the ventricle – namely, the "endocardium" in cardiac terminology – which is realistic in medical imaging practice since contrast is highest for this particular boundary. For the reference measurements we will consider three types of uncertainties to be added to the surface velocities directly inferred from the reference simulations:

1. random (Gaussian) errors, generated independently for each node of the reference mesh, for each component of the velocity and for each time step, and with standard deviation set to 20% of the reference maximum velocity value $v_{\max} = 0.17 \, \mathrm{m.s}^{-1}$;

2. spatially random shifts, namely, Gaussian errors generated indepently for each node and each component with the same standard variation, albeit constant in time;

3. modal shift, namely, a velocity profile corresponding to the trace of the first undamped eigenmode and constant in time, with an amplitude computed to give 20% of the kinetic energy norm of a constant velocity field equal to $v_{\max}$ for each component.

Note that these three types of errors are bounded in $L^2(\Gamma_m)$, as assumed in the numerical analysis. We also point out that the error amplitudes considered are quite large, as $v_{\max}$ is an upper bound of the velocity value.

4 State estimation using collocated damping

4.1 Principle

We introduce the finite dimensional state estimator of our original system (3.1)

$$\begin{cases} \dot{\bar{X}} = A\bar{X} + R + K_X(Z - H\bar{X}) \\ \bar{X}(0) = X_0 \end{cases} \tag{4.1}$$

This state estimator uses the interpolation X_0 of x_0, namely, the known part of the initial condition, and corrects the dynamics of the discrete system by a feedback proportional to the measured error. In essence, the filter K_X that we want to use corresponds to a force proportional and opposed to the measured velocity, namely a "direct velocity feedback" (DVF) stabilization strategy, see [12]. Therefore, this feedback should have the following variational form

$$-\gamma \int_{\Gamma_m} \omega \, \underline{\dot{y}} \cdot \underline{\delta y} \, d\Gamma,$$

where γ denotes a gain parameter and ω an appropriate (positive) weight function. We thus infer that K_X is the operator that takes a vector field in $L^2(\Gamma_m)$ and returns the consistent force vector obtained by using this field multiplied by $\gamma\omega$ as a surface force. Hence,

$$K_X = \begin{pmatrix} 0 \\ \gamma M^{-1}(H^v)' \end{pmatrix}, \tag{4.2}$$

where $(H^v)'$ denotes the adjoint of the *operator* H^v with respect to the weighted Γ_m-norm

$$\|\underline{\dot{y}}\|_O^2 = \int_{\Gamma_m} \omega \, (\underline{\dot{y}})^2 \, d\Gamma. \tag{4.3}$$

Moreover, defining $\bar{X} = (\bar{Y} \ \dot{\bar{Y}})^T$ we have the second order dynamics

$$M\ddot{\bar{Y}} + (C + \gamma(H^v)'H^v)\dot{\bar{Y}} + K\bar{Y} = R + \gamma(H^v)'Z, \tag{4.4}$$

with, denoting by W the matrix associated with the $\|\cdot\|_O$ norm for the degrees of freedom located on Γ_m,

$$(H^v)'H^v = (T_\Gamma)^T W T_\Gamma, \tag{4.5}$$

and this demonstrates the dissipative effect of the collocated filter.

4.2 Estimation error analysis and assessment

In order to analyse the estimation error associated with (4.1), we introduce the following discrete reference system

$$\begin{cases} \dot{X} = AX + R + K_X(\bar{Z} - HX) \\ X(0) = X_0 + \zeta_X \end{cases} \tag{4.6}$$

where ζ_X represents the interpolation of ζ_x in the finite element space. Note that this system is not the direct discretization of the continuous mechanical formulation, since it involves an additional filtering

term containing the "theoretical" measurement $\bar{Z}$. This discrete reference system is specifically defined in order to control the discretization error as seen through the observation operator, namely,

$$\epsilon_h = \mathcal{H}(x - x_h), \tag{4.7}$$

where x_h denotes the field associated with X, see Appendix for an error estimate.

We then define the state estimation error as

$$\check{X} = X - \bar{X},$$

$$\begin{cases} \dot{\check{X}} = (A - K_X H)\check{X} - K_X \chi \\ \check{X}(0) = \zeta_X \end{cases} \tag{4.8}$$

Note that ϵ_h does not appear in this error system, but it will be present in the parameter estimation stage, hence controling this term is necessary. Furthermore, using a filtered discrete reference system allows to control the state estimation error in the enhanced energy norm associated with the matrix

$$N' = N + H'H = \begin{pmatrix} \frac{K}{2} & 0 \\ 0 & \frac{M}{2} + (T_\Gamma)^T W T_\Gamma \end{pmatrix}, \tag{4.9}$$

with the corresponding norm denoted by $\|\cdot\|_{\mathcal{E}'}$.

Therefore, the estimation error analysis amounts to studying the properties of the (discrete) collocation-stabilized system (4.8). This type of problem was already discussed in details in [9]. Here we consider a boundary collocation feedback instead of the volume-distributed control employed in [9], hence we refer to [4, 7] for some specific theoretical results regarding boundary stabilization. These results establish exponential stability properties for continuous systems similar to that considered here, but do not provide quantitative estimations of stability constants. Hence, we will resort to numerical studies to compute the poles of the dynamical system (4.8), and to determine the influence of mesh discretization and feedback gain parameter on these poles to assess this stability. We emphasize that our objective is to observe the state of a system using a numerical model, hence we are primarily concerned with the stability of this numerical model to control the error in (4.8) (rather than the stability of an underlying continuous system). Nevertheless, we are also interested in assessing how this stability property may vary when changing the corresponding mesh discretization in the observer formulation, as this may be desirable to improve accuracy.

In the sequel all physical units correspond to the *SI system*. We show in Figure 4 the computed poles for $\gamma = 1.2\ 10^3$. This value is chosen so that damping for the first mode is slightly sub-critical, but this adjustment is not very sensitive and can performed in an automatic manner [9]. We can see that all the computed poles are very effectively damped by the collocated feedback – even though this feedback is boundary-concentrated and only applied on a subpart of the boundary. Namely, the corresponding time constant of the stabilization effect is found to be below 1/15 s, i.e. much smaller than the time scale of the heart beat cycle (approximately one second). Moreover, the damping is hardly affected by the discretization parameter, at least for the frequency range of concern in this type of simulation, see Table 1 for the sizes of the meshes considered.

Figure 5 demonstrates the performance of the state estimator. The initial condition error corresponds to a static displacement obtained by imposing an internal pressure of 10^3 Pa, the order of magnitude of the pressure during ventricular filling. The measurement uncertainty considered is of the above described

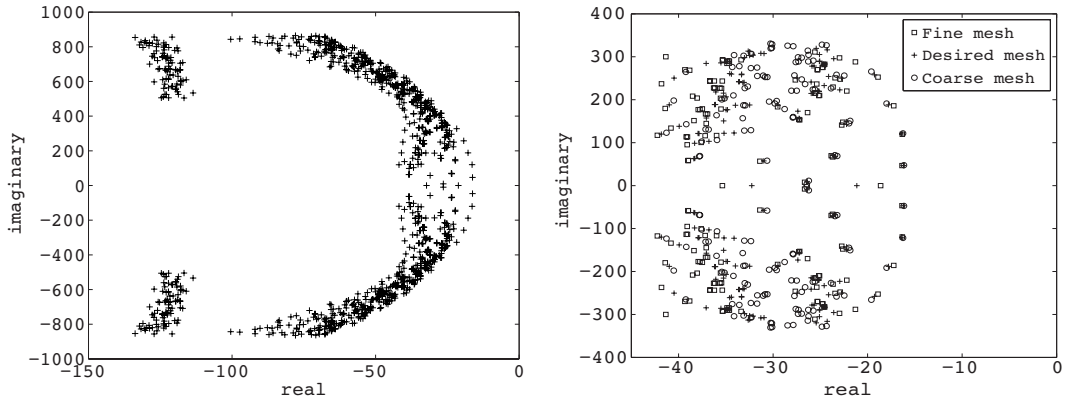

Figure 4: First 1000 poles for the desired mesh (left) and comparison for various discretizations (right, 150 modes only)

mesh	DOF ($\backsim$)
Reference	$4\ 10^4$
Fine	$2\ 10^4$
Desired	$6.5\ 10^3$
Coarse	$2.9\ 10^3$

Table 1: Number of dofs for the computational meshes

first type, but very similar results are obtained with the other types. In this figure, we compare the energy of the state estimation error with the energy (namely, given by $\|\cdot\|_{\mathcal{E}}^2$) of the reference solution and with the classical errors associated with:

- the solution of the direct problem generated with the desired mesh without initial condition error (this gives the curve labeled "discretization error")
- the reference solution interpolated in the desired mesh at each time step (the "interpolation error")

This shows that we obtain optimal accuracy of the estimation for the desired discretization – after a very short startup time corresponding to the stabilization of the collocated system – since the estimation error is then very close to the interpolation error, and indeed significantly smaller than the discretization error near the end of the time window. This is because the discretization error is associated with an "open-loop" discrete system, namely, without any data-tracking correction, unlike the collocated estimator.

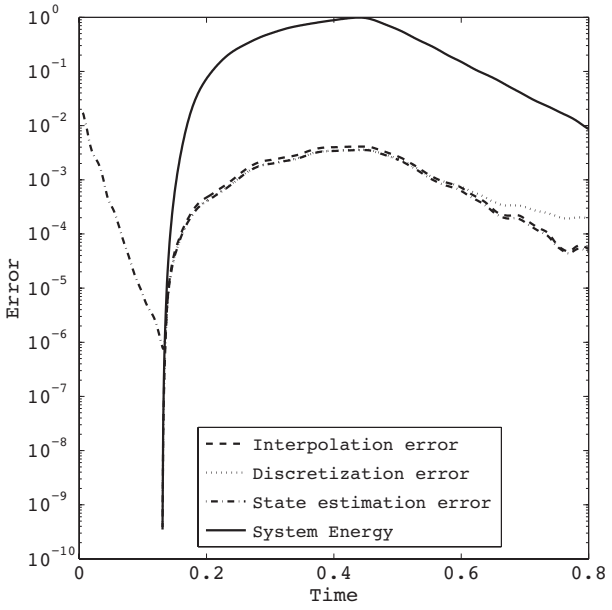

Figure 5: Comparison of estimation, discretization and estimation errors

5 Joint state-parameter estimation

5.1 Construction and analysis of the estimation procedure

Like in [9], we introduce the augmented state-parameter dynamical system, namely,

$$\begin{cases} \dot{X}^e = A^e X^e + R^e \\ X^e(0) = X_0^e + \zeta^e \end{cases} \tag{5.1}$$

where

$$X^e = \begin{pmatrix} X \\ \theta \end{pmatrix}, \quad A^e = \begin{pmatrix} A & B \\ 0 & 0 \end{pmatrix}, \quad R^e = \begin{pmatrix} R \\ 0 \end{pmatrix}, \tag{5.2}$$

and

$$X_0^e = \begin{pmatrix} X_0 \\ \theta \end{pmatrix}, \quad \zeta^e = \begin{pmatrix} \zeta_X \\ \zeta_\theta \end{pmatrix}. \tag{5.3}$$

Note that the parameter dependence considered in our model problem – recall (3.7) – is compatible with this setting, with a time-dependent B matrix. Although we do not (always) explicitly write $B(t)$, this time dependence is taken into account in the below analysis.

Of course, the augmented state vector X^e is too large for direct filtering purposes, hence we also introduce the augmented dynamics for a state equation that corresponds to the above state estimator $\bar{X}$. Defining $\bar{X}^e = (\bar{X}^T \quad \theta^T)^T$ we have

$$\begin{cases} \dot{\bar{X}}^e = A^e \bar{X}^e + R^e + K_X^e (Z - H^e \bar{X}^e) \\ \bar{X}^e(0) = X_0^e + \zeta_\theta^e \end{cases} \tag{5.4}$$

where

$$\zeta_\theta^e = \begin{pmatrix} 0 \\ \zeta_\theta \end{pmatrix}, \quad K_X^e = \begin{pmatrix} K_X \\ 0 \end{pmatrix}, \quad H^e = (H \quad 0).$$

Here we point out that $\bar{X}^e$ only depends on the initial condition ζ_θ. Hence we can define $\bar{X}^e[\xi]$ for an arbitrary initial condition $\theta(0) = \theta_0 + \xi$.

In the H^∞ framework, we seek a filter $\hat{X}^e$ that provides a prescribed performance bound $1/\beta$, namely,

$$\sup_{Z,\xi} \frac{\int_0^T \|\hat{X}^e - \bar{X}^e(\xi)\|_{S^e}^2 \, dt}{\int_0^T \|Z - H^e \bar{X}^e(\xi)\|_O^2 \, dt + \|\xi\|_{P_0^{-1}}^2} \leq \frac{1}{\beta}. \tag{5.5}$$

Here, P_0^{-1} represents a user-prescribed norm used to measure the uncertainties in the parameter space – to be combined with the measurement uncertainties in the denominator – and S^e represents the matrix used for the norm of the estimation, hence it is natural for state-parameter estimation to assume the following block-diagonal decomposition

$$S^e = \begin{pmatrix} S_X & 0 \\ 0 & S_\theta \end{pmatrix}. \tag{5.6}$$

Note that the above bound gives a guaranteed attenuation level of the estimation error with respect to arbitrary disturbances in the parameter values and in the measurements. We will show that the following observer enjoys the desired attenuation property.

$$\boxed{\begin{cases} \dot{\hat{X}} = A\hat{X} + B\hat{\theta} + R + K_X(Z - H\hat{X}) + L_X\dot{\hat{\theta}}, \quad \text{with } \hat{X}(0) = X_0 \\ \dot{\hat{\theta}} = U^{-1}L_X^T H'(Z - H\hat{X}), \quad \text{with } \hat{\theta}(0) = \theta_0 \\ \dot{L}_X = (A - K_X H)L_X + B, \quad \text{with } L_X(0) = 0 \\ \dot{U} = L_X^T H' H L_X - \beta(L_X^T S_X L_X + S_\theta), \quad \text{with } U(0) = (P_0)^{-1} \end{cases}} \tag{5.7}$$

We emphasize that the essential difference with the observer formulated in [9] lies in the dynamics of U, namely, with the "negative" term associated with β in the right-hand side. Of course, this observer system is well-posed only as long as U remains positive definite – note that the initial condition P_0 is positive definite, indeed. This induces a restriction on β, or equivalently on the time window considered, as reflected in the following result.

■ **Proposition 5.1**

Consider a given T_{max}. There exists a maximum value β^* (depending on T_{max}) such that, for any β with $0 < \beta < \beta^*$ and for any T with $0 < T \leq T_{max}$, the observer defined in (5.7) *provides the attenuation bound* (5.5).

◇ **Proof :**

We define β^* the supremum of all values of β for which the integration of U in (5.7) provides a positive definite result over the whole time interval $[0, T_{\max}]$. Then – as is classical in H^∞ theory, see e.g. [2] – we define the following cost function

$$J_T^\beta = \int_0^T \|\hat{X}^e - \bar{X}^e(\xi)\|_{S^e}^2 \, dt - \frac{1}{\beta}\Big(\int_0^T \|Z - H^e \bar{X}^e(\xi)\|_O^2 \, dt + \|\xi\|_{P_0^{-1}}^2\Big). \tag{5.8}$$

Note that ensuring the attenuation bound (5.5) is equivalent to enforcing

$$\sup_{Z,\xi} J_T^\beta \leq 0. \tag{5.9}$$

We start by defining and analysing

$$W^\beta(T) = \sup_\xi J_T^\beta, \tag{5.10}$$

namely, in this supremum we consider the measurement Z as given, hence the observer $\hat{X}^e$ is also fixed since it may only depend on the measurements. Introducing an adjoint state p^e we obtain for the maximizer in (5.10) – denoted by $\bar{X}^e_{\text{sup}}$ – the following two-point boundary value problem

$$\begin{cases} \dot{\bar{X}}^e_{\text{sup}} = A^e \bar{X}^e_{\text{sup}} + R^e + K_X(Z - H^e \bar{X}^e_{\text{sup}}) \\ \dot{p^e} + (A^e - K_X^e H^e)^T p^e = H^{e\prime}(Z - H^e \bar{X}^e_{\text{sup}}) + \beta S^e(\bar{X}^e_{\text{sup}} - \hat{X}^e) \\ \bar{X}^e_{\text{sup}}(0) = X_0^e - P_a^e(0) p^e(0) \\ p^e(T) = 0 \end{cases} \tag{5.11}$$

with

$$P_a^e(0) = \begin{pmatrix} 0 & 0 \\ 0 & P_0 \end{pmatrix}.$$

Seeking the solution in the standard form

$$\bar{X}^e_{\text{sup}}(t) = r^e(t) - P^e(t) p^e(t), \tag{5.12}$$

we obtain the following Cauchy system

$$\begin{cases} \dot{P^e} - P^e(A^e - K_X^e H^e)^T - (A^e - K_X^e H^e)P^e + P^e H^{e\prime} H^e P^e - \beta P^e S^e P^e = 0 \\ \dot{r^e} + P^e H^{e\prime} H^e r^e - (A^e - K_X^e H^e) r^e - \beta P^e S^e (r^e - \hat{X}^e) = P^e H^{e\prime} Z + R^e + K_X Z \\ P^e(0) = P_a^e(0) \\ r^e(0) = X_0^e \end{cases} \tag{5.13}$$

We recognize a Riccati equation as the first equation of this system, and it is straightforward to verify that it is satisfied by

$$P_a^e = (L_X^T \quad I_r)^T U^{-1} (L_X^T \quad I_r). \tag{5.14}$$

Therefore, $\bar{X}^e_{\text{sup}}$ is adequately characterized by (5.12) and (5.13). We define $\hat{\xi}(T)$ such that $\bar{X}^e_{\text{sup}} = \bar{X}^e(\hat{\xi}(T))$ and we now study $W^\beta(T)$ as a function of T. We have $W^\beta(0) = 0$ and

$$\begin{aligned} \frac{dW^\beta(T)}{dT} &= \frac{\partial J_T^\beta}{\partial \xi} \cdot \frac{d\hat{\xi}(T)}{dT} + \left(\|\hat{X}^e - \bar{X}^e(\hat{\xi}(T))\|^2_{S^e} - \frac{1}{\beta} \|Z - H^e \bar{X}^e(\hat{\xi}(T))\|^2_O \right)(T) \\ &= \left(\|\hat{X}^e - r^e\|^2_{S^e} - \frac{1}{\beta} \|Z - H^e r^e\|^2_O \right)(T) \end{aligned}$$

using $\bar{X}^e(\hat{\xi}(T)) = \bar{X}^e_{\text{sup}}(T) = r^e(T)$, and the stationarity of J_T^β with respect to ξ that characterizes W^β. We then infer that, for the *particular choice*

$$\hat{X}^e = r^e, \tag{5.15}$$

the derivative of $W^\beta(T)$ is always negative, hence with the initial condition $W^\beta(0) = 0$ we have

$$W^\beta(T) \leq 0, \quad \forall T. \tag{5.16}$$

Note that the choice (5.15) is allowed since it provides a recursive form for the observer $\hat{X}^e$. Furthermore, with this strategy we obviously have

$$\sup_{Z,\xi} J_T^\beta = \sup_Z W^\beta(T) \leq 0, \tag{5.17}$$

namely, the desired attenuation bound holds. Finally, it is easy to check that the equations defining $\hat{X}^e = r^e$ decompose into those in the first two lines of System (5.7).

$\diamond$

5.2 Error analysis

We now carry out the analysis of the errors defined by $\tilde{X} = X - \hat{X}$, $\tilde{\theta} = \theta - \hat{\theta}$. Note that the H^∞ performance bound (5.5) provides a direct estimation error estimate, since

$$\|Z - H^e \bar{X}^e(\zeta_\theta)\|_O^2 = \|\epsilon_h + H\check{X}\|_O^2,$$

hence,

$$\int_0^T \|\hat{X}^e - \bar{X}^e\|_{S^e}^2 \, dt \leq \frac{1}{\beta}\Big(\int_0^T \|\epsilon_h + H\check{X}\|_O^2 \, dt + \|\zeta_\theta\|_{P_0^{-1}}^2\Big) \tag{5.18}$$

However, this estimation error is time-integrated, and we are also interested in a final time estimate which will provide a stronger result for parameter estimation, since the parameters are static.

Therefore, as in [9] (see also [14]) we introduce the auxiliary quantity

$$\eta = \tilde{X} - L_X\tilde{\theta}.$$

Then

$$\begin{cases} \dot{\eta} = (A - K_X H)\eta - K_X\chi \\ \dot{\tilde{\theta}} = -U^{-1}L_X^T H' H L_X\tilde{\theta} - U^{-1}L_X^T H' H\eta - U^{-1}L_X^T H'(\epsilon_h + \chi) \\ \eta(0) = \zeta_X \\ \tilde{\theta}(0) = \zeta_\theta \end{cases} \tag{5.19}$$

We note that η follows exactly the same dissipative dynamics as the state-estimator error $\check{X}$, recall (4.8), hence the same conclusions as above hold. We now consider the dynamics of $\tilde{\theta}$, which we rewrite as

$$\dot{\tilde{\theta}} = -U^{-1}L_X^T H' H L_X\tilde{\theta} + U^{-1}L_X^T H'\varrho,$$

with

$$\varrho = -(H\eta + \epsilon_h + \chi).$$

We have

$$\begin{aligned} \frac{d}{dt}(\tilde{\theta}^T U\tilde{\theta}) &= 2\tilde{\theta}^T U\dot{\tilde{\theta}} + \tilde{\theta}^T \dot{U}\tilde{\theta} \\ &= -\tilde{\theta}^T(L_X^T H' H L_X + \beta(L_X^T S_X L_X + S_\theta))\tilde{\theta} + 2\tilde{\theta}^T L_X^T H'\varrho, \end{aligned}$$

taking into account the dynamics of U given in (5.7). Integrating this equation, we infer

$$\|\tilde{\theta}(t)\|^2_{U(t)} \leq \|\zeta_\theta\|^2_{P_0^{-1}} + 2\int_0^t \tilde{\theta}^T L_X^T H' \varrho \, d\tau. \tag{5.20}$$

Defining $\lambda_U(t)$ as the smallest solution of the generalized eigenvalue problem

$$U(t)\,\xi = \lambda U(0)\,\xi,$$

we obtain from (5.20)

$$\lambda_U(t)\|\tilde{\theta}(t)\|^2_{P_0^{-1}} \leq \|\zeta_\theta\|^2_{P_0^{-1}} + 2\int_0^t (\lambda_U(\tau))^{\frac{1}{2}} \|\tilde{\theta}(\tau)\|_{P_0^{-1}} (\lambda_U(\tau))^{-\frac{1}{2}} \|L_X^T H' \varrho\|_{P_0} \, d\tau,$$

hence a direct application of the Gronwall inequality yields

$$(\lambda_U(t))^{\frac{1}{2}} \|\tilde{\theta}(t)\|_{P_0^{-1}} \leq \|\zeta_\theta\|_{P_0^{-1}} + \int_0^t (\lambda_U(\tau))^{-\frac{1}{2}} \|L_X^T H' \varrho\|_{P_0} \, d\tau. \tag{5.21}$$

Therefore we need to bound λ_U from below. For a given $T_{\max}$, we choose β_1 with $0 < \beta_1 < \beta^\star$ for $\beta^\star$ as provided by the theorem, and we define U_1 as the solution of

$$\dot{U}_1 = L_X^T H' H L_X - \beta_1 (L_X^T S_X L_X + S_\theta), \quad \text{with } U_1(0) = (P_0)^{-1}.$$

The condition $0 < \beta_1 < \beta^\star$ ensures that U_1 is positive definite over $[0, T_{\max}]$. Considering now any β such that $0 < \beta \leq \beta_1$ and the corresponding U, we have

$$\frac{d}{dt}(U - U_1) = (\beta_1 - \beta)(L_X^T S_X L_X + S_\theta), \tag{5.22}$$

hence

$$U(t) = U_1(t) + (\beta_1 - \beta)\int_0^t (L_X^T S_X L_X + S_\theta)\, d\tau, \tag{5.23}$$

and since $U_1(t)$ is positive definite

$$\lambda_U(t) \geq (\beta_1 - \beta)\lambda_{\inf,1}(t), \tag{5.24}$$

where $\lambda_{\inf,1}(t)$ is the smallest solution of the generalized eigenproblem

$$\Big(\int_0^t (L_X^T S_X L_X + S_\theta)\, d\tau\Big)\xi = \lambda U(0)\,\xi. \tag{5.25}$$

Likewise, from

$$\frac{d}{dt}\Big(U - \frac{\beta}{\beta_1} U_1\Big) = \frac{\beta_1 - \beta}{\beta_1} L_X^T H' H L_X, \tag{5.26}$$

we infer

$$\lambda_U(t) \geq \frac{\beta_1 - \beta}{\beta_1}(1 + \lambda_{\inf,2}(t)), \tag{5.27}$$

where $\lambda_{\inf,2}(t)$ is the smallest solution of the generalized eigenproblem

$$\Big(\int_0^t L_X^T H' H L_X \, d\tau\Big)\xi = \lambda U(0)\,\xi. \tag{5.28}$$

Gathering (5.24) and (5.27) – and since they hold for any $\beta_1 < \beta^\star$ – we have

$$\boxed{\lambda_U(t) \geq \max\Big((\beta^\star - \beta)\lambda_{\inf,1}(t)\ ,\ \frac{\beta^\star - \beta}{\beta^\star}(1 + \lambda_{\inf,2}(t))\Big).} \tag{5.29}$$

Note that $\lambda_{\inf,1}(t)$ grows at least in $O(t)$ due to the S_θ term in the integral, while the growth of $\lambda_{\inf,2}(t)$ is related to a "persistent excitation property", see e.g. [14].

The rest of the error estimation follows the same main lines as in [9], except that we will use the enhanced energy norm associated with N', instead of the standard energy. The sensitivity matrix L_X obeys the same dynamics as the damped state, hence it is stable. More specifically, we have a bound of the following type, for any set of parameters,

$$\|L_X(t)\theta\|^2_{\mathcal{E}'} \leq C \int_0^t \|B(\tau)\theta\|^2_{RHS}\, d\tau, \tag{5.30}$$

where $\|\cdot\|_{RHS}$ denotes an adequate norm for the right-hand side of the mechanical system equation. Defining the following natural norms for L_X and B

$$\|L_X\|_L = \sup_{\|\theta\|_{U(0)}=1} \|L_X\theta\|_{\mathcal{E}'}, \quad \|B\|_B = \sup_{\|\theta\|_{U(0)}=1} \|B\theta\|_{RHS}, \tag{5.31}$$

we thus obtain

$$\|L_X(t)\|^2_L \leq C \int_0^t \|B(\tau)\|^2_B\, d\tau. \tag{5.32}$$

We can now analyse the effect of the small contributions contained in ϱ. We have (see [9] for the details)

$$\|L_X^T H' \varrho\|_{P_0} \leq \|L_X(\tau)\|_L \|H\eta + \epsilon_h + \chi\|_O \leq \|L_X(\tau)\|_L \left(\|\eta\|_{\mathcal{E}'} + \|\epsilon_h\|_O + \|\chi\|_O\right), \tag{5.33}$$

hence, in (5.21) bounding by 1 the term $(\lambda_U(\tau))^{-\frac{1}{2}}$ in the integral – recall (5.29) – we infer

$$\boxed{\|\tilde\theta(t)\|_{P_0^{-1}} \leq (\lambda_U(t))^{-\frac{1}{2}}\Big(\|\zeta_\theta\|_{P_0^{-1}} + \|L_X\|_{L^2([0,t];L)}\big(\|\eta\|_{L^2([0,t];\mathcal{E}')} + \|\epsilon_h\|_{L^2([0,t];O)} + \|\chi\|_{L^2([0,t];O)}\big)\Big).} \tag{5.34}$$

This bound, together with

$$\boxed{\|\eta\|_{L^2([0,t];\mathcal{E}')} \leq C\Big(\sqrt{T_1}\|\zeta_X\|_{\mathcal{E}} + \sqrt{t}\,(\gamma\sqrt{T_2}\|\chi\|_{L^2([0,t];O)} + \varepsilon)\Big),} \tag{5.35}$$

and (5.29) provide a complete error estimate for parametric estimation.

Finally, the error bound for state estimation is simply deduced from the identity $\eta = \tilde X - L_X\tilde\theta$, namely,

$$\boxed{\|\tilde X\|_{\mathcal{E}'} \leq \|\eta\|_{\mathcal{E}'} + \|L_X\|_L \|\tilde\theta\|_{P_0^{-1}}.} \tag{5.36}$$

We now show the numerical results obtained with our estimation procedure for the above-described test problem. In all our simulations we keep the parameter γ as chosen in Section 4 for the collocated feedback. The parameter norm matrix at initial time is defined by $P_0^{-1} = 1/17\, I$ to ensure that the variation of each scalar parameter is $O(1)$. Since the objective of the H^∞ filter is parameter identification – state estimation being handled by the collocated filter – we choose $S_X = 0$, and without any other *a priori*

knowledge on the identifiability of the system we take $S_\theta = P_0^{-1}$. For the time discretization of the estimator, we use the classical prediction-correction scheme corresponding to the discrete H^∞ formulation of our system.

Figure 6 displays the estimated parameters for the first type of uncertainties with $\beta = 0$, which means that our filter then corresponds to the reduced-order Kalman procedure proposed in [9]. We can see that the 17 scalar values of contractilities are quite accurately – and rapidly, once contraction occurs – recovered, including for the reduced value in the "infarcted" region number 14. This is to be compared with the results shown in Figure 7 and corresponding to $\beta = 5$, a value close to the maximum allowed to retain invertibility of U during the time window considered, as was determined by numerical experiments. This figure reveals significantly increased sensitivity for parameter estimation, which is to be expected since U is decremented by the H^∞ contribution, recall (5.7). Note that this increased sensitivity is particularly large for region 17 – a region with almost no direct measurement, hence of likely reduced identifiability for the contractility parameter.

Similar results are obtained for the other 2 types of uncertainties, see Figure 8. Nevertheless, the parameter estimation is less effective in the third case, which was to be expected since the corresponding uncertainty is a shift with a mode, hence it is *biased* and contains some *physical* features not accounted for in the measurement modeling.

Finally, we show in Figure 9 the estimation results for two different values of β – namely, $\beta = 2$ and $\beta = 5$ – considering the third (modal) type of uncertainty, to be compared with the results for $\beta = 0$ in Fig.8. Beyond the already discussed increased sensitivity effect, we observe no improvement in the estimation when increasing β. This is in apparent contradiction with the H^∞ approach – since $1/\beta$ represents the performance bound, recall (5.5) – but this numerical result is consistent with the *final time* estimate (5.34), as (5.29) provides the largest lower bound for $\lambda_U(t)$ when $\beta = 0$. Of course, the contradiction is only apparent since the H^∞ criterion uses a *time-integrated* estimation error. In fact, in our numerical tests we have also found that the error bound provided by the H^∞ criterion – namely, (5.18) – is numerically too large to be of any practical value, unlike the final time error.

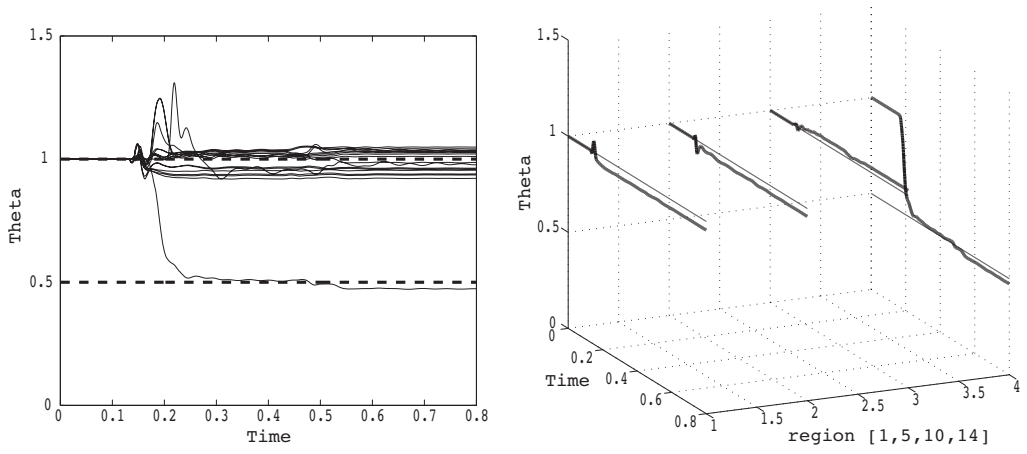

Figure 6: Uncertainties of first type with $\beta = 0$: estimated values for all 17 parameters (left) and for 4 individual regions (right)

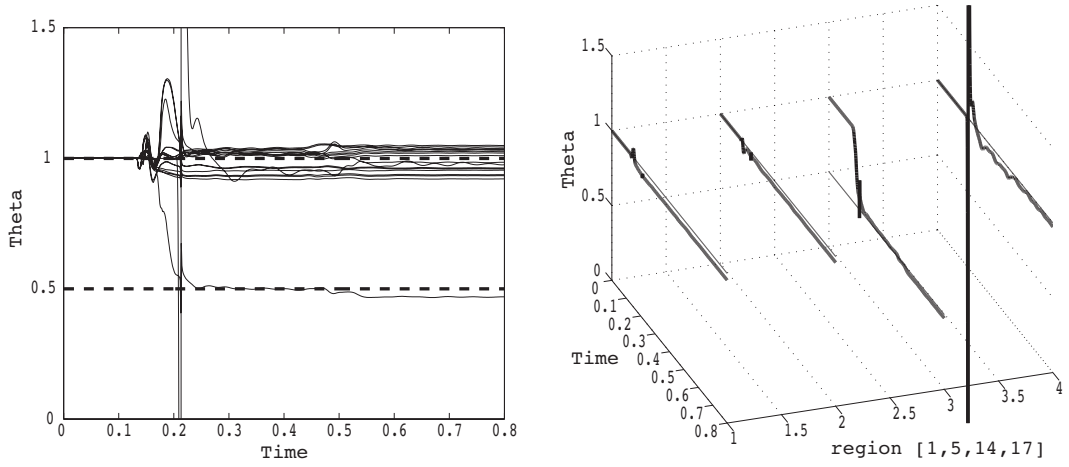

Figure 7: Uncertainties of first type with $\beta = 5$: estimated values for all 17 parameters (left) and for 4 individual regions (right)

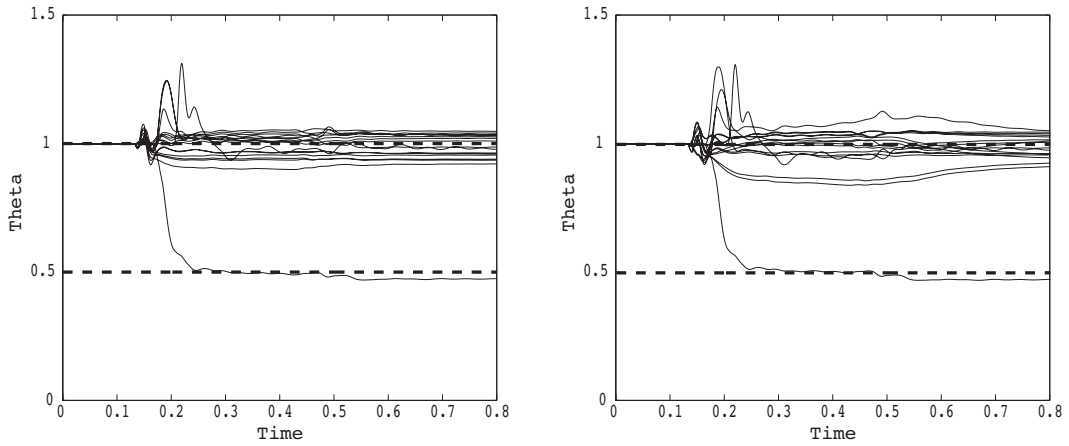

Figure 8: Uncertainties of second (left) and third (right) types with $\beta = 0$: estimated values for all 17 parameters

6 Concluding remarks

We have presented a reduced-rank filtering procedure for joint state-parameter estimation in distributed mechanical systems. This procedure was formulated in the spirit of the method proposed in [9] – namely, using a collocated feedback strategy for effective state estimation – albeit in an H^∞ framework, which differs in theory from the optimal filtering approach adopted in [9]. Nevertheless, this leads to quite similar recursive filter equations, with an additional term parametrized by the H^∞ performance bound.

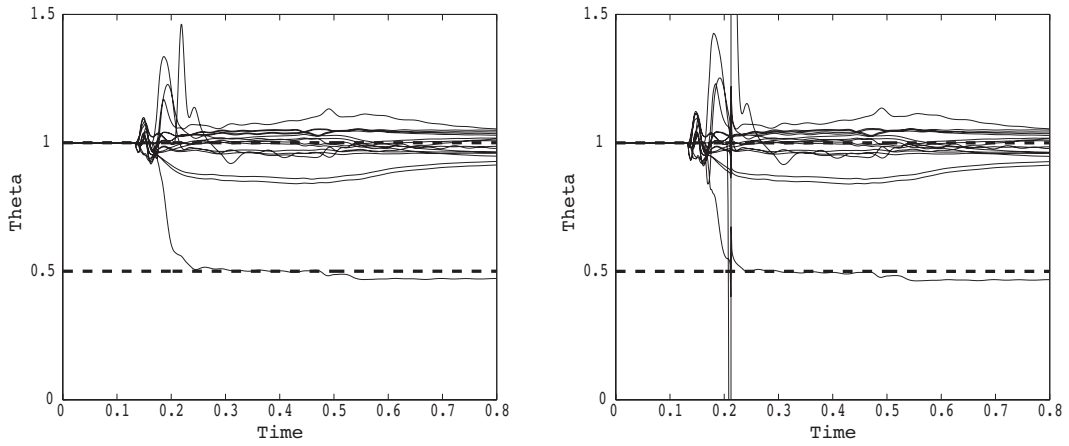

Figure 9: Uncertainties of third type with $\beta = 2$ (left) and $\beta = 5$ (right): estimated values for all 17 parameters

Considering a test problem inspired from cardiac biomechanics, our numerical tests have demonstrated the excellent performance of the state estimation with a collocated filter using only velocity measurements concentrated in a subregion of the boundary. This is a particularly interesting result, since boundary measurements cannot be analysed in an optimal filtering setting, as boundary white noise loading leads to unbounded mean energy in mechanical systems, in general.

In addition, we have obtained complete final time error estimates for the state-parameter estimation procedure in the case when the joint state-parameter system is linear, namely, when the parameters enter in the loading of a linear mechanical system.

Furthermore, we have performed detailed numerical assessments of the joint estimation procedure, using the cardiac test problem and seeking the values of some parameters representing tissue contractilities, medical diagnosis assistance being an important potential application for this type of procedure. For the three types of measurement uncertainties considered, the parameter values were recovered quite accurately, the best results being obtained when discarding the additional H^∞ term (namely, $\beta = 0$). This was found to be in agreement with the final time error estimates obtained in the numerical analysis. In this limit case $\beta = 0$, we have formally the same filter equations as in [9], albeit the H^∞ approach provides an adequate setting for considering some types of measurement errors that cannot be dealt with in the Kalman framework.

Finally, we point out that various extensions of this filtering procedure can be formulated for *nonlinear* state-parameter systems as proposed in [9], in particular by using either an "extended-Kalman" or an "unscented-Kalman" approach [6, 13].

References

[1] AHA/ACC/SNM. Standardization of cardiac tomographic imaging. *Circulation*, 86:338–339, 1992.

[2] T. Başar and P. Bernhard. *H^∞-Optimal Control and Related Minimax Design Problems - A Dynamic Game Approach*. Birkhaüser, 2nd edition, 1995.

[3] K.J. Bathe. *Finite Element Procedures*. Prentice Hall, 1996.

[4] S. Cox and E. Zuazua. The rate at which energy decays in a string damped at one end. *Indiana Univ. Math. J.*, 44(2):545–573, 1995.

[5] T.J.R. Hughes. *The Finite Element Method : Linear Static and Dynamic Finite Element Analysis*. Prentice Hall, 1987.

[6] S. Julier and J. Uhlmann. Unscented filtering and nonlinear estimation. In *Proceedings of the IEEE*, volume 92, 2004.

[7] G. Lebeau and L. Robbiano. Stabilisation de l'équation des ondes par le bord. *Duke Math. J.*, 86(3):465–491, 1997.

[8] L. Ljung. *Theory and Practice of Recursive Identification*. MIT Press, 1983.

[9] P. Moireau, D. Chapelle, and P. Le Tallec. Joint state and parameter estimation for distributed mechanical systems. *Computer Methods in Applied Mechanics and Engineering*, 197:659–677, 2008.

[10] Z. Pan and T. Başar. Parameter identification for uncertain linear systems with partial state measurements under an H-infinity criterion. *IEEE Transactions on Automatic Control*, AC-41:1295–1311, 1996.

[11] D.T. Pham, J. Verron, and M.C. Roubeaud. A singular evolutive interpolated Kalman filter for data assimilation in oceanography. *J. Marine Systems*, 16:323–341, 1997.

[12] A. Preumont. *Vibration Control of Active Structures, An Introduction*. Kluwer Academic Publishers, 2nd edition, February 2002.

[13] M. Wu and A.W. Smyth. Application of the unscented Kalman filter for real-time nonlinear structural system identification. *Struct. Control Health Monit.*, 14:971–990, 2006.

[14] Q. Zhang and A. Clavel. Adaptive observer with exponential forgetting factor for linear time varying systems. In *Proceedings of the 40th IEEE Conference on Decision and Control*, volume 4, pages 3886–3891, Orlando, FL, USA, 2001.

A Error estimate for $(x - x_h)$

In the derivation of this estimate, we start from state equations without internal damping. Structural damping could also be considered – at the expense of lengthier expressions but without deep modifications – and would lead to enhanced estimates, indeed.

We recall that the variational formulations satisfied by the continuous and discrete displacements are

$$\int_\Omega \rho \ddot{\underline{y}} \cdot \delta\underline{y}\, d\Omega + \int_\Omega \underline{\underline{\varepsilon}}(\underline{y}) : C : \delta\underline{\underline{\varepsilon}}\, d\Omega = \int_\Omega \underline{f} \cdot \delta\underline{y}\, d\Omega, \quad \forall \delta\underline{y}, \tag{A.1}$$

$$\int_\Omega \rho \ddot{\underline{y}}_h \cdot \delta\underline{y}_h\, d\Omega + \int_\Omega \underline{\underline{\varepsilon}}(\underline{y}_h) : C : \delta\underline{\underline{\varepsilon}}\, d\Omega = \int_\Omega \underline{f} \cdot \delta\underline{y}_h\, d\Omega + \gamma(\mathcal{H}^v(\dot{\underline{y}} - \dot{\underline{y}}_h), \mathcal{H}^v(\delta\underline{y}_h))_O, \quad \forall \delta\underline{y}_h. \tag{A.2}$$

In (A.2) we denote by $(\cdot,\cdot)_O$ the scalar product associated with the O-norm.

We now define Π_h as the projection operator from the continuous to discrete displacement spaces for the $(\cdot,\cdot)_{\rm St}$ scalar product. Namely, in particular,

$$\int_\Omega \underline{\underline{\varepsilon}}(\Pi_h \underline{y}) : C : \delta\underline{\underline{\varepsilon}}\, d\Omega = \int_\Omega \underline{\underline{\varepsilon}}(\underline{y}) : C : \delta\underline{\underline{\varepsilon}}\, d\Omega, \quad \forall \delta \underline{y}_h. \tag{A.3}$$

Subtracting (A.2) from (A.1) and using $(\Pi_h \underline{\dot{y}} - \underline{\dot{y}}_h)$ as a test function, we thus obtain

$$\begin{aligned}\frac{d}{dt}\|\Pi_h \underline{\dot{y}} - \underline{\dot{y}}_h\|^2_{\rm In} + \frac{d}{dt}\|\Pi_h \underline{y} - \underline{y}_h\|^2_{\rm St} + \gamma\|\mathcal{H}^v(\Pi_h \underline{\dot{y}} - \underline{\dot{y}}_h)\|^2_O \\ = 2(\Pi_h \underline{\ddot{y}} - \underline{\ddot{y}}, \Pi_h \underline{\dot{y}} - \underline{\dot{y}}_h)_{\rm In} + \gamma(\mathcal{H}^v(\Pi_h \underline{\dot{y}} - \underline{\dot{y}}), \mathcal{H}^v(\Pi_h \underline{\dot{y}} - \underline{\dot{y}}_h))_O,\end{aligned} \tag{A.4}$$

where we denote by $(\cdot,\cdot)_{\rm In}$ and $(\cdot,\cdot)_{\rm St}$ the scalar products induced by the inertia and stiffness bilinear forms, respectively, and by $\|\cdot\|_{\rm In}$ and $\|\cdot\|_{\rm St}$ the corresponding norms. Of course, these norms are equivalent to the L^2 and H^1 norms, respectively. Using the standard inequality

$$|(\mathcal{H}^v(\Pi_h \underline{\dot{y}} - \underline{\dot{y}}), \mathcal{H}^v(\Pi_h \underline{\dot{y}} - \underline{\dot{y}}_h))_O| \le \frac{1}{2}(\|\mathcal{H}^v(\Pi_h \underline{\dot{y}} - \underline{\dot{y}})\|^2_O + \|\mathcal{H}^v(\Pi_h \underline{\dot{y}} - \underline{\dot{y}}_h)\|^2_O),$$

we infer

$$\begin{aligned}\frac{d}{dt}\|\Pi_h \underline{\dot{y}} - \underline{\dot{y}}_h\|^2_{\rm In} + \frac{d}{dt}\|\Pi_h \underline{y} - \underline{y}_h\|^2_{\rm St} + \frac{\gamma}{2}\|\mathcal{H}^v(\Pi_h \underline{\dot{y}} - \underline{\dot{y}}_h)\|^2_O \\ \le 2(\Pi_h \underline{\ddot{y}} - \underline{\ddot{y}}, \Pi_h \underline{\dot{y}} - \underline{\dot{y}}_h)_{\rm In} + \frac{\gamma}{2}\|\mathcal{H}^v(\Pi_h \underline{\dot{y}} - \underline{\dot{y}})\|^2_O.\end{aligned} \tag{A.5}$$

This implies

$$\frac{d\mathcal{E}_h}{dt} \le 2(\Pi_h \underline{\ddot{y}} - \underline{\ddot{y}}, \Pi_h \underline{\dot{y}} - \underline{\dot{y}}_h)_{\rm In} + \frac{\gamma}{2}\|\mathcal{H}^v(\Pi_h \underline{\dot{y}} - \underline{\dot{y}})\|^2_O,$$

with

$$\mathcal{E}_h(t) = \|\Pi_h \underline{\dot{y}} - \underline{\dot{y}}_h\|^2_{\rm In} + \|\Pi_h \underline{y} - \underline{y}_h\|^2_{\rm St},$$

and we can use the Gronwall inequality to obtain

$$\mathcal{E}_h(t)^{\frac{1}{2}} \le \left\{\mathcal{E}_h(0) + \int_0^t \frac{\gamma}{2}\|\mathcal{H}^v(\Pi_h \underline{\dot{y}} - \underline{\dot{y}})\|^2_O\, d\tau\right\}^{\frac{1}{2}} + \int_0^t \|\Pi_h \underline{\ddot{y}} - \underline{\ddot{y}}\|_{\rm In}\, d\tau. \tag{A.6}$$

Therefore,

$$\boxed{\mathcal{E}_h(t) \le 2\mathcal{E}_h(0) + \int_0^t \gamma\|\mathcal{H}^v(\Pi_h \underline{\dot{y}} - \underline{\dot{y}})\|^2_O\, d\tau + 2t\int_0^t \|\Pi_h \underline{\ddot{y}} - \underline{\ddot{y}}\|^2_{\rm In}\, d\tau,} \tag{A.7}$$

and using again (A.5) we also have for the measurement error

$$\boxed{\gamma\|\mathcal{H}^v(\Pi_h \underline{\dot{y}} - \underline{\dot{y}}_h)\|^2_O \le C\Big\{\gamma\|\mathcal{H}^v(\Pi_h \underline{\dot{y}} - \underline{\dot{y}})\|^2_O + \|\Pi_h \underline{\ddot{y}} - \underline{\ddot{y}}\|^2_{\rm In} + \|\Pi_h \underline{\dot{y}} - \underline{\dot{y}}_h\|^2_{\rm In}\Big\}.} \tag{A.8}$$

Of course, in order to obtain similar estimates for $(\underline{y} - \underline{y}_h)$ we need to invoke bounds on the projection error $(\underline{y} - \Pi_h \underline{y})$ in the same norms. As the projection is defined as the discrete solution of a standard linearized elasticity problem – recall (A.3) – such bounds are classical and only depend on the regularity of the domain and of the loading. We finally point out that ϵ_h can be bounded – as neeeded in the estimates of Section 5.2 – using (A.8) as we have

$$\|\epsilon_h\|_{W^{-1}} \le C\|\epsilon_h\|_O \le C\Big(\|\mathcal{H}^v(\Pi_h \underline{\dot{y}} - \underline{\dot{y}}_h)\|_O + \|\mathcal{H}^v(\Pi_h \underline{\dot{y}} - \underline{\dot{y}})\|_O\Big). \tag{A.9}$$